Ni-YSZ films deposited by reactive magnetron sputtering for SOFC applications

Ekaterina Rezugina, Anne-Lise Thomann, Hervé Hidalgo, Pascal Brault, Vincent Dolique, Yves Tessier

Ni-YSZ films deposited by reactive magnetron sputtering for SOFC applications

E. Rezugina(*), A.L. Thomann, H. Hidalgo, P. Brault(*), V. Dolique, Y. Tessier

Groupe de Recherches sur l'Energétique des Milieux Ionisés, UMR6606-CNRS, 14 rue d'Issoudun, BP 6744, 45067 Orléans Cedex 2, France

(*) rezugina@gmail.com; Pascal.Brault@univ-orleans.fr

Abstract

Ni-YSZ films are deposited by reactive magnetron sputtering from a single Ni/Zr/Y metallic target at rates as high as 4µm.h^{-1}. Tailoring both DC pulsed power and oxygen partial pressure, a stable deposition process was obtained. Columnar morphology was observed in the as-deposited films. Annealing in air at 900°C was conducted, after which a fully crystallized structure was achieved. Chemical composition has been measured by Rutherford Backscattering Spectroscopy (RBS) and Nuclear Reaction Analysis (NRA). To find optimal conditions for reactive deposition of the films, effect of oxygen flow rate on the discharge parameters was studied. Film deposition onto glass substrates was carried out to measure electrical conductivity.

1. Introduction

Solid Oxide Fuel Cells are of big interest nowadays and are becoming one of the main competitors among environmental friendly energy sources for the future due to low emission rates, high electric efficiency and a potential for a low operating cost [1]. A fuel cell is a device for direct conversion of chemical energy into electrical energy. It consists of three various kinds of materials exhibiting different properties: a cathode, an anode, and an electrolyte. The oxidant (O_2 or air) is fed to the cathode, and fuel (H_2 or hydrocarbon) to the anode. The electrolyte, through which the ion current flows, also prevents the mixing of oxidant and fuel. At present, conventionally designed SOFCs operate at a relatively high temperature, between 800°C and 1000°C [2], which limits their field of application (problem of material thermal stability). SOFCs working at intermediate temperatures (i.e. below 700°C) could thus reduce operating cost, increase durability, and extend service life. Different researches are involved to meet the requirements needed for the SOFC temperature reduction, such as novel materials [3, 4] fabrication methods [5-7] or design of cell components [8].

Conventional fuel cells use dense yttria-stabilized zirconia (YSZ) as the electrolyte, porous nickel cermet (Ni-YSZ) for the anode, and porous strontium- doped lanthanum manganite (LSM) as the cathode. Ni-YSZ with a 50 vol % Ni has been employed as the anode for its reasonable cost, good catalytic activity and electrical conductivity.

Fuel cell efficiency depends on the resistive and polarisation losses which are ohmic resistance of the electrolyte and reaction resistance of the electrode. Lowering of the electrolyte thickness leads to the reduction of the resistive losses through the electrolyte, which allows operating at lower temperatures. A porous electrode with a sufficient electronic conductivity is necessary for cell operation. The porous structure provides electrochemical reactions across the electrode.

In this study, the conventional materials have been chosen and the reduction of SOFC operating temperature is expected from the thin film technology implemented for the cell components. The synthesis of thin electrolyte and electrodes by magnetron sputtering method [9, 10] can provide required films properties and be relevant for mass market application. Magnetron sputtering is a plasma deposition technique which is often used for thin films deposition; it permits to control density and composition of the films even for low thicknesses (from nm to μm scale)

This article describes plasma sputtering fabrication process of the Ni-YSZ thin films. Chemical composition and structural properties are characterized. Influence of oxygen pressure on plasma processing parameters and thin films properties is considered. Electrical conductivity is measured for four different film compositions.

2. Experiment

The films of Ni-YSZ were deposited on silicon (100) substrates by magnetron reactive sputtering. The magnetron sputtering system (APRIM Vide), with three independent planar magnetron targets, has been described elsewhere [11]. The target used for the electrode deposition is a Ni/Zr/Y (68.8/26.6/4.6 wt % and 99.9% purity) alloy. The expected film composition is $Ni_{0.6}((Y_2O_3)_{0.2}(ZrO_2)_{0.8}))_{0.4}$. The targets were 4 inches in diameter and placed 90 mm away from the substrate. The Ni/Zr/Y metal target was powered by a pulsed DC power supply (Pinnacle+, Advanced Energy). The DC power was varied in the range 400-1000W to obtain sufficient deposition rates and expected film properties. The pulse frequency was 100 kHz with 2.2μs duration of a positive voltage (22% of the negative bias). Similar deposition technique has already been reported in [12-16]. The maximum deposition rate of the Ni-YSZ samples reached in this work is $4\mu m.h^{-1}$. All coatings were deposited for 20-30 minutes according to the desired film thickness. Before the process, the deposition chamber

was evacuated using a turbomolecular pump to a pressure of $2 \cdot 10^{-6}$ mbar. Argon at 40 sccm flow and oxygen at 2-7 sccm flow were introduced into the system. A working pressure in the range $2 \cdot 10^{-3}$ mbar to $10 \cdot 10^{-3}$ mbar was maintained during the deposition by controlling the pumping speed and keeping the gas flow rates constant. Before the deposition, the target surface was sputtered for 3-5 min to remove oxidized layer and contaminants while the substrate was protected. Oxygen flow, total pressure and DC power were tuned to investigate the deposition condition effects on the film properties. The substrates were placed on a rotating holder to obtain films of uniform composition and thickness. Afterwards some samples were annealed at 900 °C for 90 min in air to improve their crystalline quality. The annealing conditions were chosen based on previous studies found in the literature [17].

The structures of the films were characterized by θ-2θ X-Ray Diffraction using a Philip's diffractometer (X'Pert Pro: PW 1830 generator, CRMD, Orleans), with CuK_{α} radiation (λ=1.54184 Å) at 40 kV/30mA. The Nuclear Reaction Analysis (NRA) used for oxygen concentration measurements, was carried out on a Van de Graff accelerator (CEMHTI, Orleans) with 900keV deuton beam. The corresponding nuclear reaction on oxygen is $^{16}O(d,\alpha)^{14}N$. Ta_2O_5 was the reference sample for oxygen density calibration. The chemical composition of the samples was studied by Rutherford Backscattering Spectroscopy (RBS). These measurements were carried out in the same equipment as NRA using a 2000 keV $^{4}He^{+}$ ion beam. The NRA and RBS spectra were simulated using the SIMNRA code [18]. The surface morphology and film thickness were studied by a Scanning Electron Microscope (SEM) (Carl Zeiss SMT, Supra-40, FEG-SEM).

A two probe method (Microworld S-302-4, Signatone S-725-SLM) was applied for measuring electrical conductivity of the films with different oxygen contents. The measurements were carried out at room temperature in a longitudinal mode.

3. Results and discussion

3.1. Reactive sputtering study

Before deposition, plasma characterization has been performed to investigate the effect of oxygen on the sputtering process efficiency. In Figure 1, the discharge voltage development as a function of oxygen flow is displayed. It is known that the deposition rate during reactive magnetron sputtering strongly depends on the target surface conditions. The target can become oxidized (poisoned) by the oxygen which reduces the amount of sputtered material. Therefore the oxygen flow has to be precisely controlled for better results. Hysteresis development observed in Fig. 1 was studied as a function of the oxygen flow in order to obtain reproducible deposition rates and film properties. Ar partial pressure was fixed to $5 \cdot 10^{-3}$ mbar and the oxygen flow was increased from 0 sccm to 10 sccm, (constant Ar flow =40 sccm). As can be seen from Figure 1, until nearly 6 sccm, the discharge voltage stays high. This region defines the metallic mode. Above 6 sccm discharge voltage starts to fall and later stabilizes. This means the process enters the oxide mode, for which deposition rate can be noticeably lower and even might be zero. In this region, target is oxidized and the secondary electron emission coefficient is higher compare to the metallic mode, resulting in an increased discharge current and a falling voltage at a constant value of power (here 500 and 700W) [9].

From the hysteresis curves (Figure 1), we define three deposition conditions. Corresponding deposition rates and chemical compositions are presented in Table 1.

3.2. Film characteristics

3.2.1 Chemical composition

Figure 2 shows experimental RBS spectrum of Sample 1 and its simulated SIMNRA [17] spectrum. This RBS spectrum displays two peaks corresponding, from the left to the right, to Si substrate, Ni and Y+Zr elements in the film. Because the molar masses of Y and Zr

elements are too close, their RBS peaks are overlapped, so their contents are presented as the sum Y+Zr. These peaks can be fitted by changing the overall composition and the layer thickness. Oxygen concentration was measured by NRA and the results were included in the RBS simulation to fit the composition of the film using the correct amount of oxygen. Simulating the elemental concentration according to each layer, one can directly obtain the actual concentration in the thin film. Three oxygen peaks can be observed on the NRA spectrum given in Figure 3, and the corresponding reactions are $^{16}O(d,\alpha)\ ^{14}N$, $^{16}O(d,p_1)^{17}O$ and $^{16}O(d,p_0)^{17}O$. The last peak belongs to the carbon, which comes from the organic contamination of the top layer. The corresponding C amount is typical of handled samples.

The composition of Sample 1 is closer to the expected values; also the deposition rate is higher compared to the other two samples: this suggests that these deposition conditions could be considered as optimal. Oxygen content is noticeably higher in Sample 2 and 3; since (Y+Zr) fraction is quite low, this shows that Ni is partly oxidized. It is seen from Sample 3 that, in our experimental conditions, the deposition rate remains high even at the beginning of the oxide mode. The results show that annealing in air roughly doubled the oxygen content, which led to a chemical composition closer to the expected one. Figure 4 shows oxygen content in the films as a function of oxygen flow rate during deposition. It is seen that the oxygen content increases and only depends on the flow rate; it seems to be unaffected by power changes.

3.2.2 *Morphology*

Figure 5 displays SEM images of the top surface and cross-section of Ni-YSZ thin film Sample 1. The as-deposited film surface (top view) exhibits granular morphology with small grains of 10nm slightly replicating a cauliflower-like structure. On all samples, bumps of 100nm with hemispherical shape are observed.

The cross-section reveals that the cauliflower-like structures are emerging from a columnar structure, which is expected for magnetron sputtering deposition [19]. The same morphology was seen in all Ni-YSZ deposited samples.

Evolution of surface and cross-sectional morphology after annealing at 900°C for 90 min can be observed in Fig 5c-d. Ni-YSZ film after annealing has a denser structure due to atomic reorganisation during heat treatment. The cross-section is no longer columnar and grains and boundaries are less distinguished. The thickness (1160nm) of the film after annealing remains unchanged. The dense structure obtained after annealing is not favourable to the application, since porous layers are required for SOFC electrodes. Nevertheless, the porosity should be recovered by the shrinkage occurring during the nickel oxide reduction that takes place in usual cell operation conditions (hydrogen atmosphere).

3.2.3 Crystalline structure

Figure 6 presents XRD patterns of Sample 1. Before annealing the pattern has one broad peak and one small hump. Clearly the film exhibits a poor crystalline quality. After annealing sharp diffraction peaks corresponding to the diffraction of 8YSZ, NiO(200), Ni(111) planes are detected. The positions of the NiO peaks are in agreement with those for the NiO standards. XRD shows that the films after annealing have improved crystalline structure with clear indicated peaks. Based on the XRD results it is possible to identify the broad peaks present in the as-deposited film as corresponding to the disordered phases of YSZ and NiO and/or Ni.

From the results given above, optimum deposition conditions can be discussed. Accurate values of oxygen amounts can be obtained (but with a loss of Zr +Y) on the as deposited films (Sample 2) for high deposition rates. However, the films are not well crystallized, which may be damaging for their properties. The best results should be obtained by performing the film

deposition at a low oxygen flow rates, which ensures the highest deposition rates, but leads to a lack of oxygen that can be controlled. This would be corrected by the oxidizing effect during the annealing step.

3.3. Test of Electrical properties

Even if the required characteristics are reached (oxygen content, crystallized phases), it is important to check the film properties. Electrical conductivity of the films (samples 0 to 3) with different oxygen content deposited onto glass substrates was investigated by the two probe method. The results, given in table 2, indicate that the presence of oxygen leads to a decrease of the electrical conductivity, which can reach zero.

Comparing to some previous results based on the sol-gel technique [23], for which at room temperature a conductivity of 0.1 $10^4 \cdot S.cm^{-1}$ is reported, the obtained values are favourable. This suggests that a part of Ni in some of the as-deposited films is not oxidized. Since in ref [23] samples have been H_2 reduced before electrical measurements, it means that plasma sputtering leads to very efficient Ni conducting networks in the films. This value of electrical conductivity will be further improved by NiO reduction to Ni in the hydrogen atmosphere during cell operation.

4. Conclusions

It has been shown that pulsed DC magnetron reactive sputtering can be an efficient technique to obtain thin conductive films of complex oxides such as Ni-YSZ with deposition rates of 4 $\mu m.h^{-1}$. The annealing step needed for the film crystallization has been found to increase the global oxygen content. Study of the deposition conditions versus oxygen flow rate has allowed evidencing an optimal way to synthesize crystalline films with a chemical composition close to the theoretical one. The conditions giving the best properties of the films

will be used to deposit the SOFC anode for further annealing in H_2 for reducing NiO. Moreover this technique will be used to assemble a complete SOFC by depositing its electrodes and an electrolyte using magnetron sputtering only.

Acknowledgements

This work has been partly funded by Conseil Régional Région Centre

The authors would like to express their acknowledgment to the partners who have contributed to the study: Alain Pineau (CRMD, CNRS Orléans) for the XRD measurements and Thierry Sauvage (CERI/CEMTHI, CNRS Orléans) for the RBS and NRA experiments.

References

[1] M.C. Williams, Fuel Cells. **1,** 87-91 (2001)

[2] Z. Yang, International Materials Reviews **53 (**2008) 39-54

[3] A. Tarancon, Stephen J. Skinner, Richard J. Chater, F. Hernandez-Ramirez and J. A. Kilner, J. Mater. Chem. **17**, 3175 (2007)

[4] W.Z. Zhu, S.C. Deevi, Materials Science and Engineering **A362**, 228-236 (2003)

[5] G. Shiller, R. Henne, M. Lang and M. Muller, Fuel Cells **4**, 1-2 (2004)

[6] A. Ringuede, J.A. Labrincha, J.R. Frade, Solid State Ionic **141-142**, 549-557 (2001)

[7] L.R. Pederson, P. Singh, X.-D. Zhou, J. Vacuum **80**, 1066-1083 (2006)

[8] D. Rotureau, J.-P. Viricelle, C. Pijolat, N. Caillol and M. Pijolat, Journal of the European Ceramic Society 25 (2005) 2633-2636

[9] P. J. Kelly, R. D. Arnell, J. Vacuum **56**, 159-172 (2000)

[10] I. Safi, Surface and Coatings Technology **127**, 203-219 (2000)

[11] C. Wang, P. Brault, C. Zaepffel, J. Thiault, A. Pineau, T. Sauvage, J. Phys. D:Appl. Phys. **36**, 2709-2713 (2003)

[12] P. Yashar, J. Rechner, M.S. Wong, W.D. Sproul, S.A. Barnett, J. Surface and Coating Tehcnology **94-95**, 333-338 (1997)

[13] T. Tsai, Scott A. Barnett, J. Electrochem. Soc. **5**, 145 (1998)

[14] A. Billard, D. Mercs, F. Perry, C. Frantz, Surface and Coatings Technology **140**, 225-230 (2001)

[15] A. Belkin and Z. Zhao, in *Proceeding of 43d Annual Technical Conference, Denver*, Society of Vacuum Coaters, (2000), p. 86

[16] D. Carter, D. Madsen and W.D. Sproul, Advanced Energy Industries, Inc. (2003)

[17] Shyankay Jou, Tzu-Hui Wu, J. Physics and Chemistry of Solids **69**, 2804-2812 (2008)

[18] M. Mayer 1997 SIMNRA user's guide, IPP 9/113 (Garching: Max-Planck-Institut fur Plasma Physik) SIMNRA homepage http://www.rzg.mpg.de/~mam

[19] Handbook of Deposition Technologies for Films and Coatings: Science, Technology and Applications, 2nd Ed. Rointan F. Bunshah, ed., Noyes Publications (1994)

[20] JCPDS- International Centre for Diffraction Data, Powder Diffraction File No. 30-1468, 2000

[21] JCPDS- International Centre for Diffraction Data, Powder Diffraction File No. 47-1049, 2001

[22] JCPDS- International Centre for Diffraction Data, Powder Diffraction File No. 04-0850, 2001

[23] F.H. Wang, R.S. Guo, Q.T. Wei, Y. Zhou, H.L. Li, S.L. Li, Materials Letters **58**, (2004) 3079-3083

Tables

Table 1: Comparison of the properties of the 4 samples (for Ar flux 40 sccm, input power 700W, Ar pressure $5 \cdot 10^{-3}$ mbar).

	O_2 (sccm)	Deposition rate ($\mu m.h^{-1}$)	as-deposited			after annealing		
			Ni	O	Y+Zr	Ni	O	Y+Zr
Expected values			31	47	22			
Sample 0	0.4	3.8	69	10	21			
Sample 1	2	3.5	40	30	30	21	56	23
Sample 2	5	3.4	41	50	9			
Sample 3	8	3.0	35	58	7			

Table 2: Electrical conductivity measured at room temperature on 4 samples before annealing.

	Oxygen concentration at. %	Electron Conductivity $S.cm^{-1}$
Sample 0	10	$3 \cdot 10^4$
Sample 1	30	$1 \cdot 10^4$
Sample 2	50	0
Sample 3	58	0

Figures captions

Fig. 1. Discharge voltage evolution as a function of oxygen flow rate under constant power 500 and 700 W, $5 \cdot 10^{-3}$ mbar. The three deposition conditions with different oxygen flow rates are shown in the experimental curve.

Fig. 2. RBS experimental and simulated spectra of Sample 1.

Fig. 3. NRA spectrum and SIMNRA simulation of Sample 1.

Fig. 4. Oxygen content in the films as a function of oxygen flow rate. Total pressure $5 \cdot 10^{-3}$ mbar, Ar flow rate 40 sccm

Fig. 5. SEM observations of Sample 1 as deposited (a, b) and after annealing at 900°C for 90min in air (c, d)

Fig. 6. XRD patterns of NiO-YSZ film (Sample 1), before and after annealing in air at 900°C for 90 min. Peaks references [20-22].

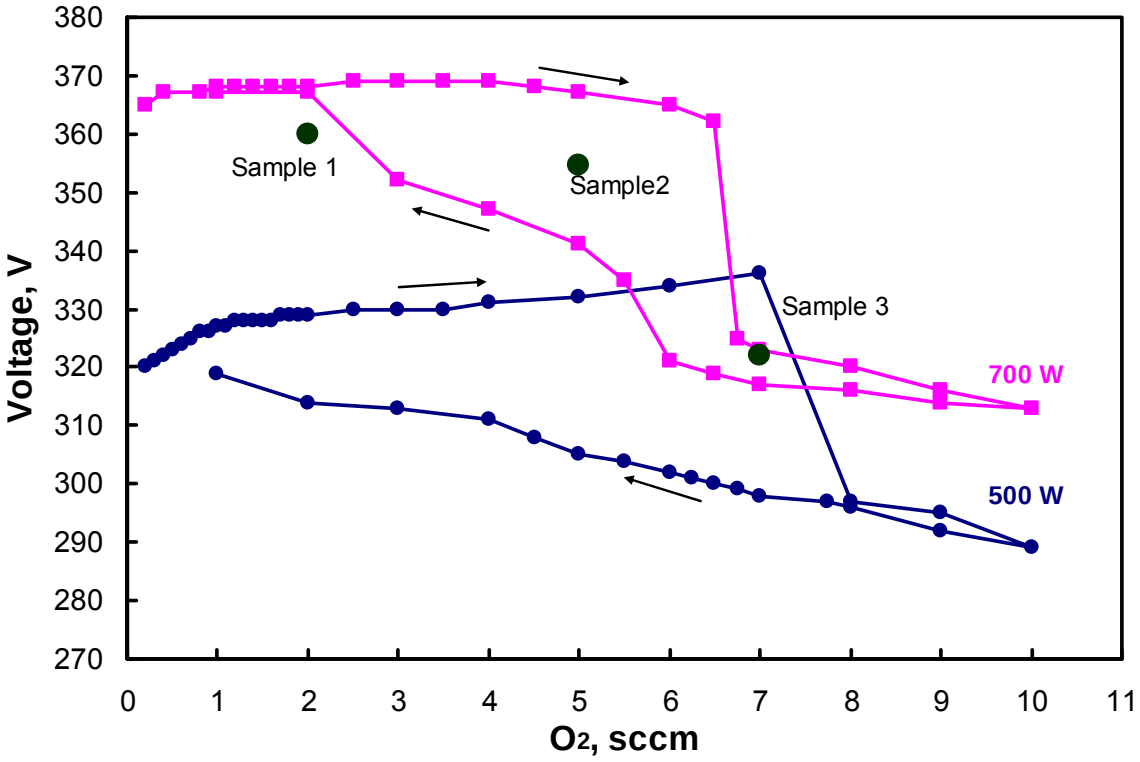

Fig. 1

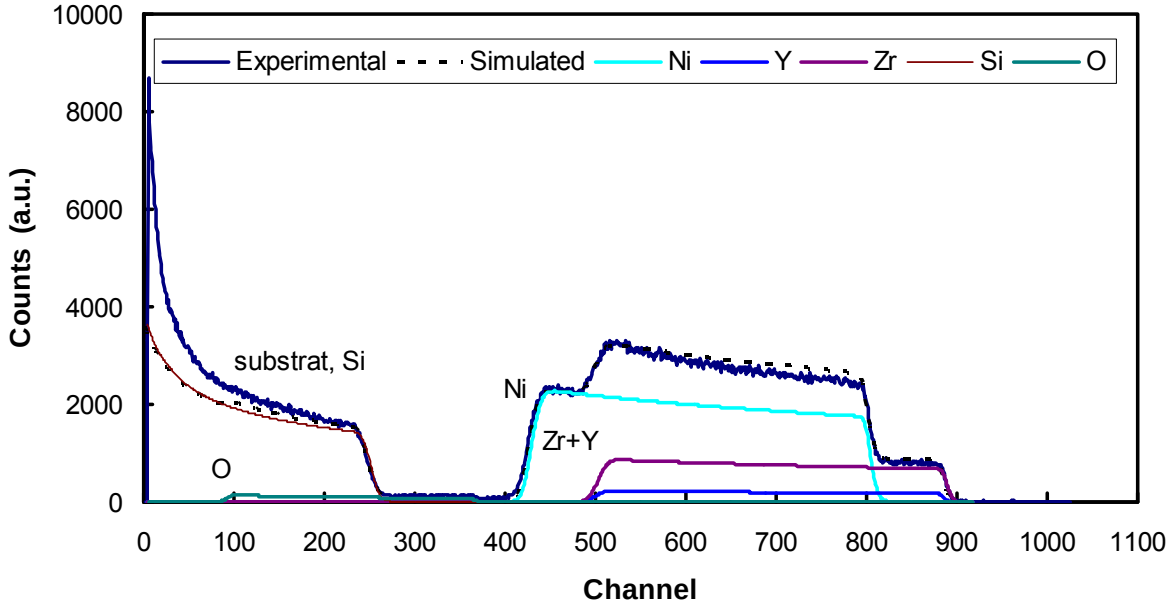
Experimental
Simulated
Ni
Y
Zr
Si
O
Counts (a.u.)
Channel
substrat, Si
Ni
Zr+Y
O
10000
8000
6000
4000
2000
0
0
100
200
300
400
500
600
700
800
900
1000
1100

Fig.2

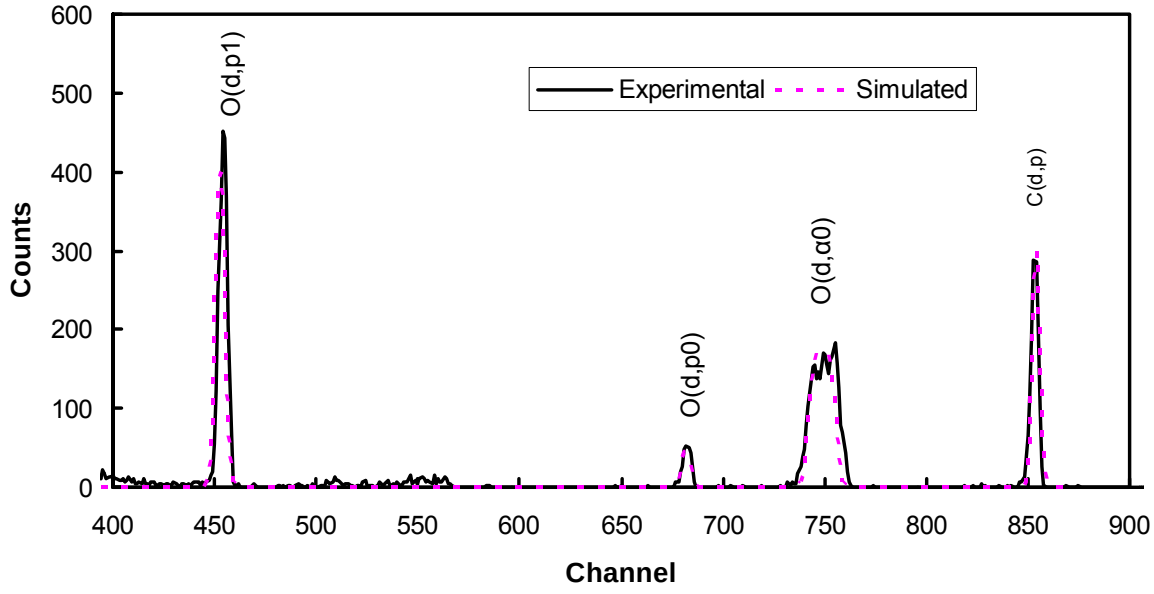
600
500
400
300
200
100
0
Counts
O(d,p1)
O(d,p0)
O(d,α0)
C(d,p)
Experimental
Simulated
400
450
500
550
600
650
700
750
800
850
900
Channel

Fig. 3

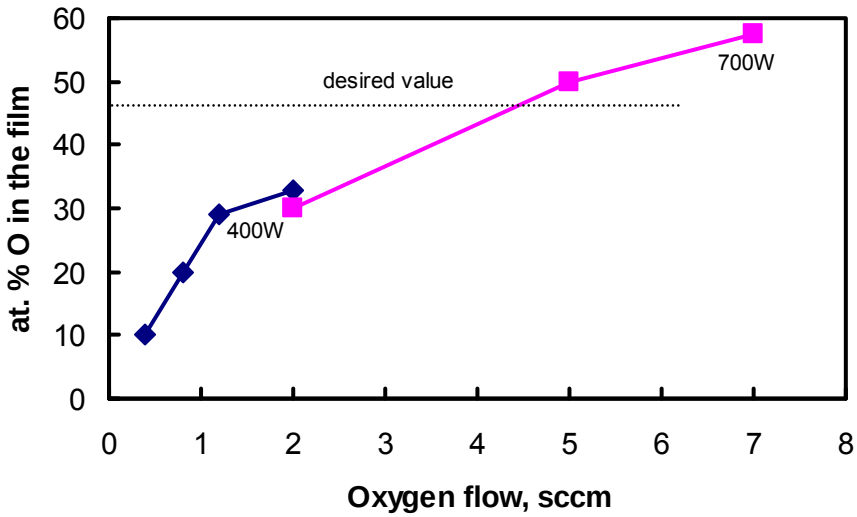
60
50
40
30
20
10
0
at. % O in the film
desired value
700W
400W
0
1
2
3
4
5
6
7
8
Oxygen flow, sccm

Fig. 4

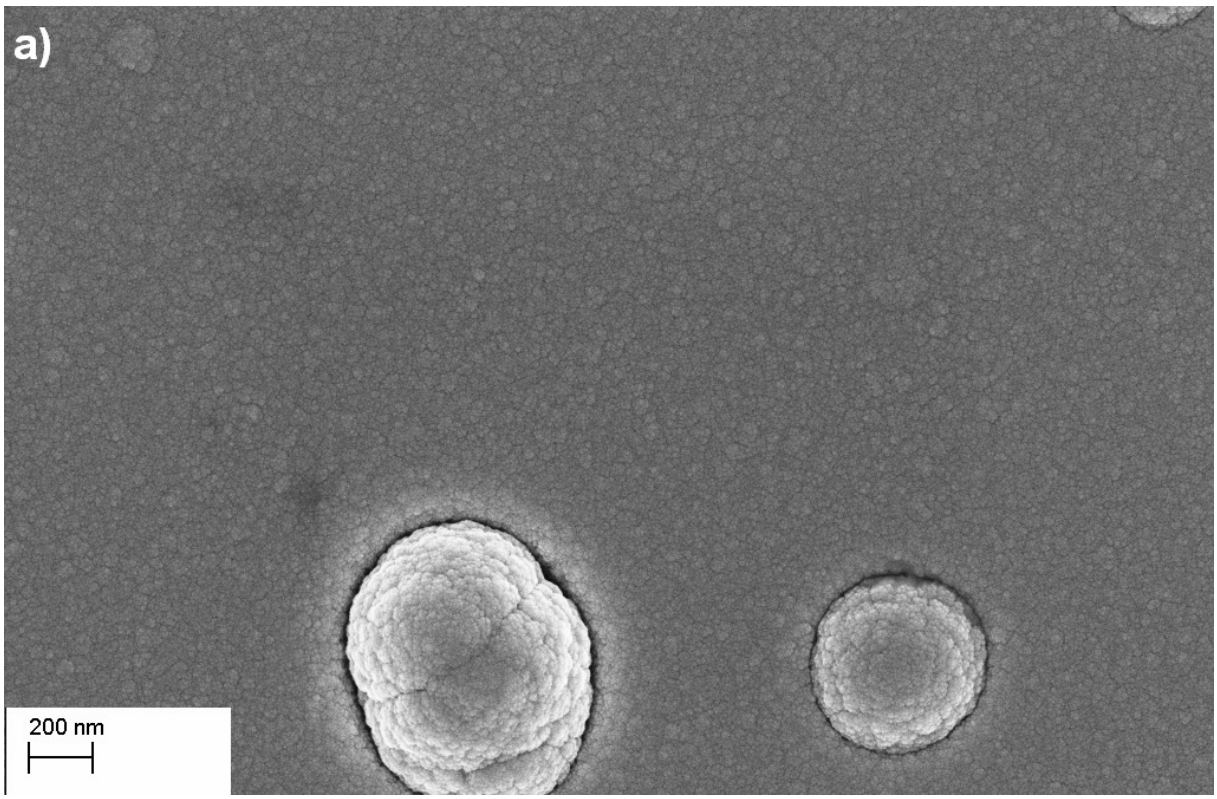

Fig. 5a

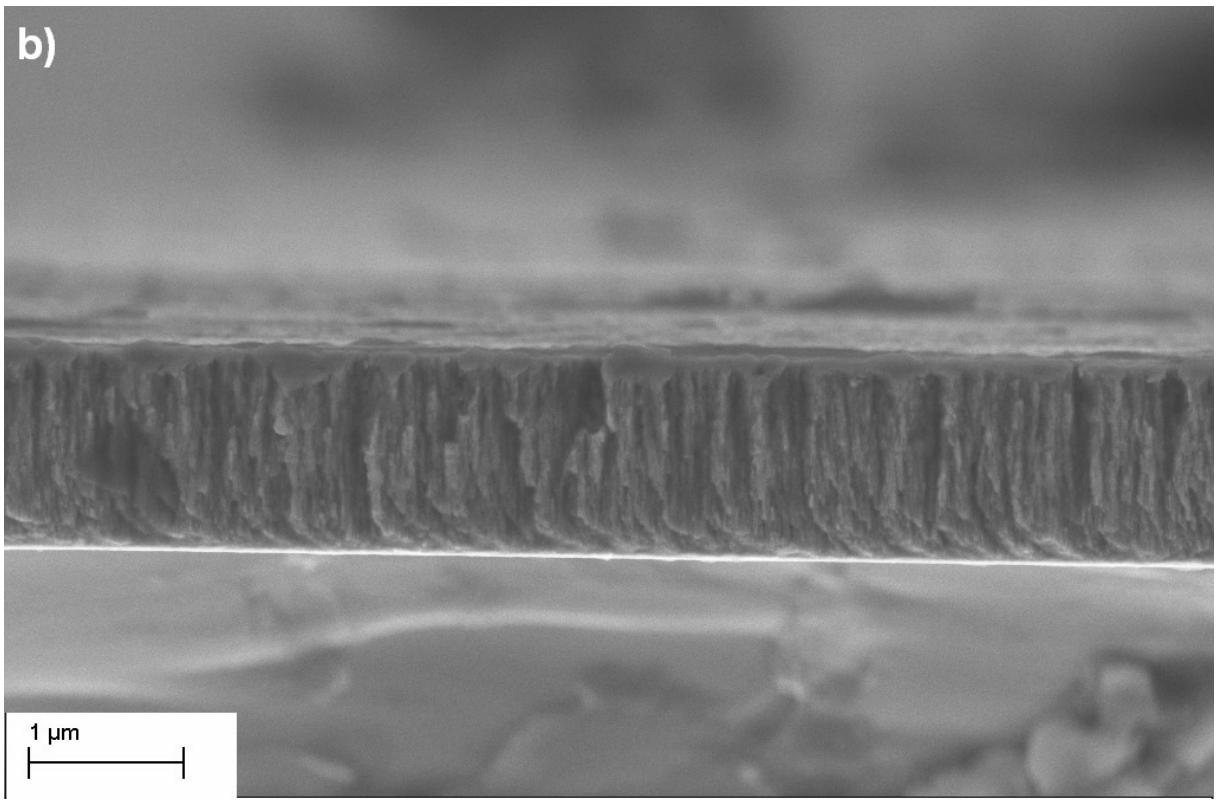

Fig. 5b

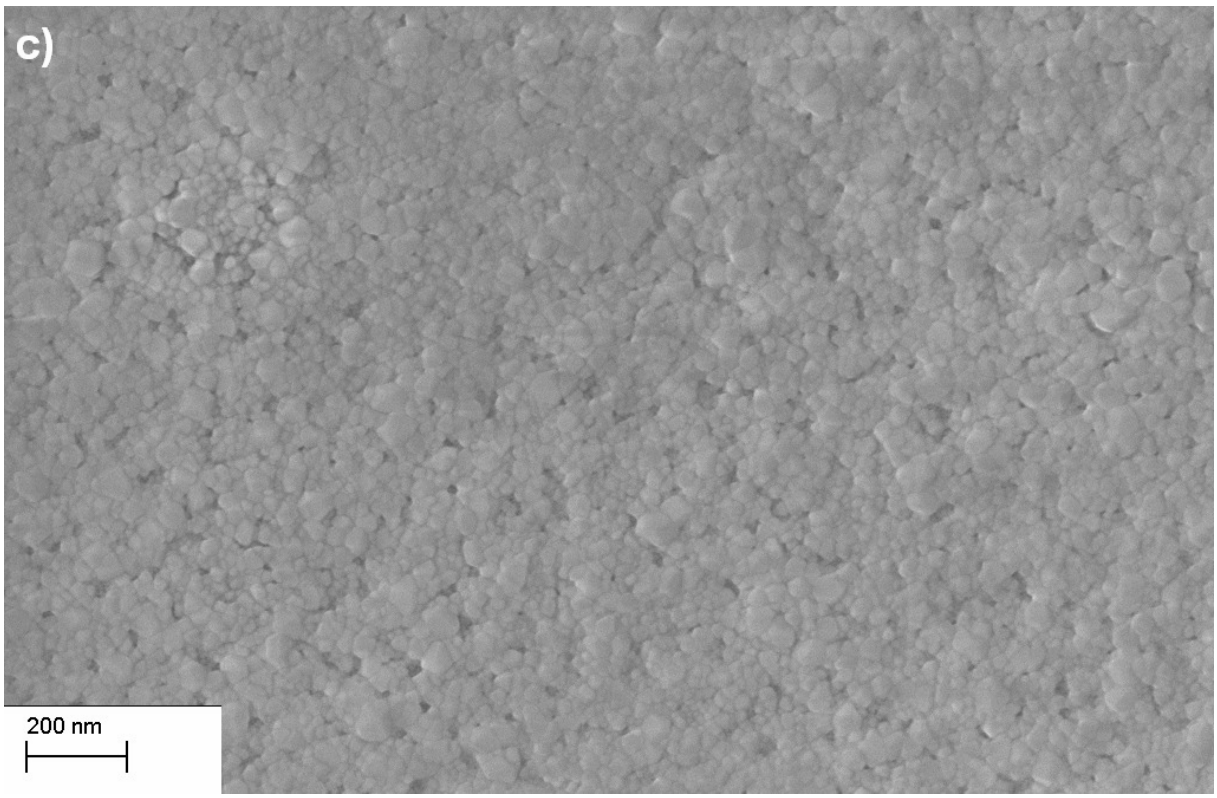

Fig. 5c

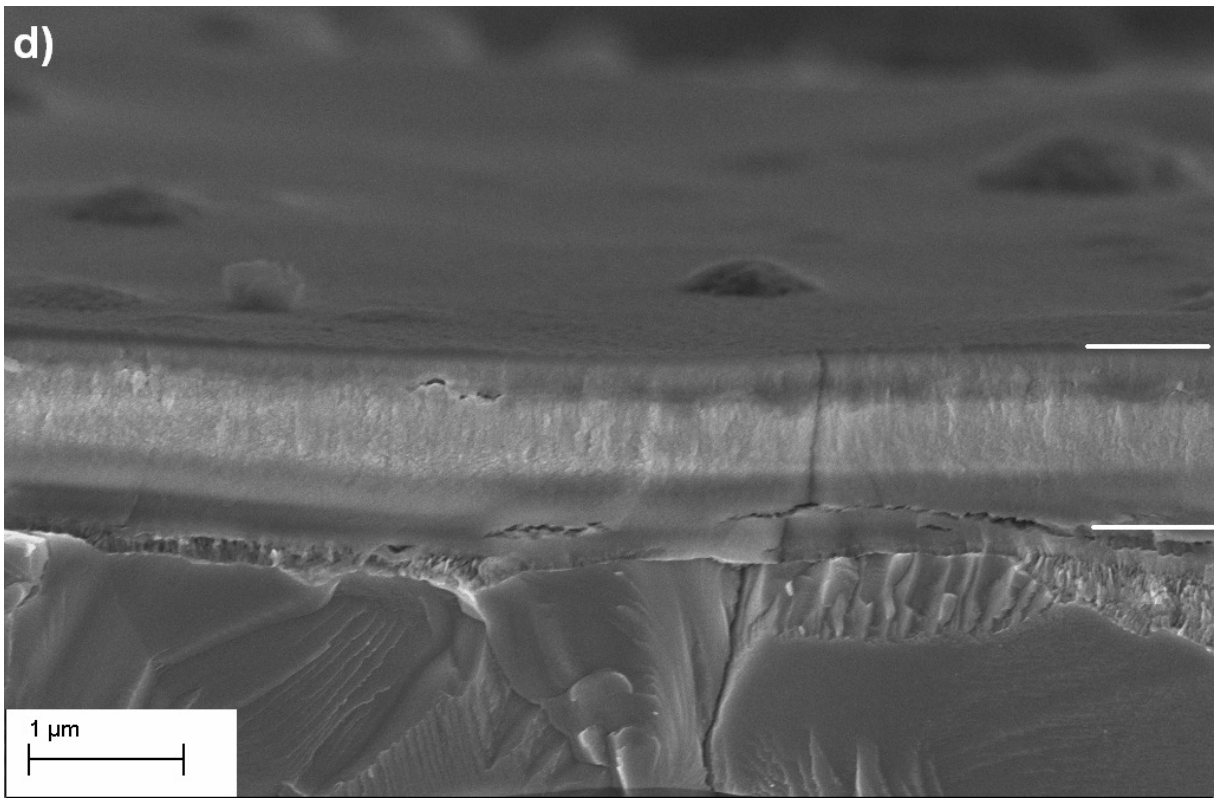

Fig.5d

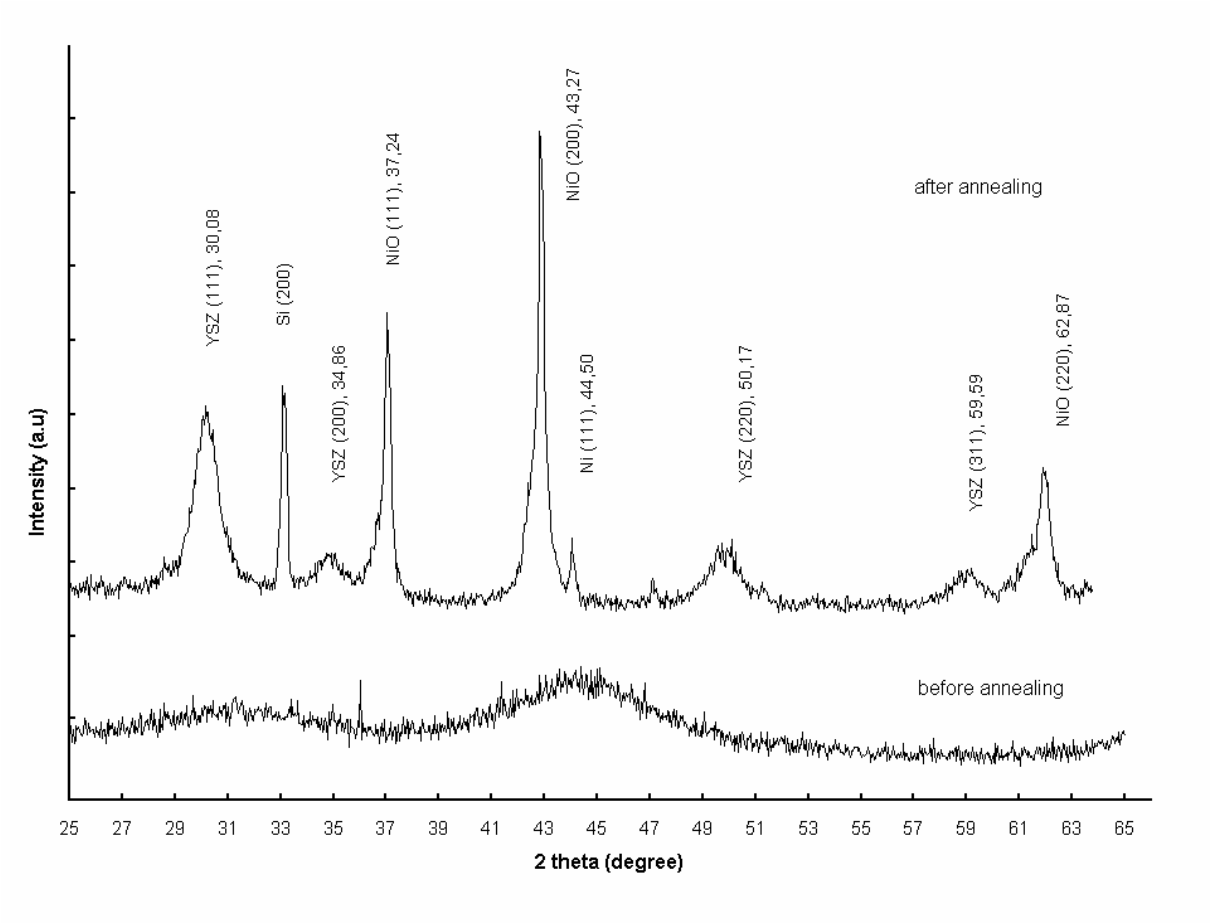
YSZ (111), 30,08
Si (200)
YSZ (200), 34,86
NiO (111), 37,24
NiO (200), 43,27
Ni (111), 44,50
YSZ (220), 50,17
YSZ (311), 59,59
NiO (220), 62,87
after annealing
before annealing
Intensity (a.u)
25 27 29 31 33 35 37 39 41 43 45 47 49 51 53 55 57 59 61 63 65
2 theta (degree)

Fig. 6